A COMPREHENSIVE WEAR MODEL FOR CUTTING TOOLS
Technical Report No. UM-MEAM-88-5

Tsu-Ren Ko, Research Assistant
and
Yoram Koren, Professor

1 General approach

In order to estimate tool wear from the cutting force measurement, it is necessary to understand the relationship between tool wear and the cutting force. Tool wear is usually categorized into two types : crater wear on the rake surface, and clearance wear that includes flank and nose wears.

2 The clearance wear model

The relationship between the cutting force and flank wear has been studied by several researchers [1-3]. Their works were mainly based on the investigations of either orthogonal cutting or oblique cutting. Basically, they assumed certain pressure distribution and constant friction coefficient on the flank wear surface. Usually in both orthogonal and oblique cuttings, the width of the flank wear, W_f, develops uniformly and the change of the cutting force ,$\triangle\vec{F}$, may be modeled as :

$$\triangle\vec{F} = \vec{F}_p + \vec{F}_f \tag{1}$$

where $\vec{F}_p$ and $\vec{F}_f$ are two perpendicular components given by

$$\vec{F}_p = P_{av}\, W_f\, b \tag{2}$$

and

$$\vec{F}_f = \mu\, P_{av}\, W_f\, b \tag{3}$$

where P_{av} is the average pressure on the flank wear surface, b is the width of cut (or the depth of cut in turning), and μ is the friction coefficient. Note that $\vec{F}_p$ acts normal inward to the flank wear surface and $\vec{F}_f$ acts along the direction of the cutting speed.

In the case of real turning applications, the tool engagement is more complex, since the insert nose is also involved in the cutting operations. We can, however, extend the flank wear model to the nose surface and obtain a comprehensive wear model that describes the change of the cutting force due to clearance wear.

Let us define s as the coordinate along the projection of the actual cutting edge on the plane perpendicular to the cutting speed with the starting point corresponding to the initial cutting point on the flank edge and the ending point to the end cutting point on the nose edge, as shown in Fig. 1. The change of the cutting force due to pressure on the clearance wear surface can be written as

$$\vec{F}_p = \int_0^{s_2} \int_0^{W(s)} p(s,w)\, \vec{n}\,(s)\, dw\, ds, \tag{4}$$

where $W(s)$ is the local wear at point s, $p(s,w)$ is the pressure distribution on the clearance wear surface, $\vec{n}(s)$ is the unit normal vector pointing inward on the clearance wear surface, and s_2 is the value of the ending point in the s coordinate. Note that since we analyze a general turning case in which the tool is tilted with respect to the workpiece, the wear, W, is measured along the direction of the cutting speed and may not be perpendicular to the cutting edge. $\vec{F}_p$ in Eq. (4) represents a force that its direction varies with $\vec{n}$ along s. Also note that Eq. (2) is a particular case of the comprehensive model of Eq. (4), in which $W(s)$ becomes a constant, W_f, and s is a straight line of a length b.

The general expression of the force change due to the friction force on the clearance wear surface may be written as :

$$\vec{F}_f = \int_0^{s_2} \int_0^{W(s)} \mu(s,w)\, p(s,w)\, \vec{v}\, dw\, ds, \tag{5}$$

where $\mu(s,w)$ is the friction coefficient on the clearance wear surface and $\vec{v}$ is the unit tangent vector in the direction of the cutting speed. The sum of these two forces represents the total cutting force change due to clearance wear.

To evaluate Eqs. (4) and (5), the following functions should be known :

1. $p\,(s,w)$
2. $\mu\,(s,w)$
3. $\vec{n}\,(s)$
4. $W\,(s)$.

To know the exact structures of these functions is very complex in machining. However, as a first approximation, we can make assumptions regarding the above four functions to simplify the model.

By assuming that the average pressure on the clearance wear surface is constant [1], we have :

$$[\int_0^{W(s)} p(s,w)\, dw]\,/W(s) = P_{av}(s) = P_{av} = constant. \tag{6}$$

By assuming that the friction coefficient on the clearance wear surface remains unchanged, we have :

$$\mu(s, w) = \mu = constant. \tag{7}$$

By assuming that clearance wear does not change the original shape of the cutting edge (viewed from the direction of the cutting speed), we obtain :

$$\vec{n}(s) = \vec{n_o}(s) \tag{8}$$

where $\vec{n_o}$ is the unit vector normal to the cutting speed pointing inward to the cutting edge of an unworn tool. Finally, we assume that clearance wear may be written in an approximate linear form (see Fig. 2) as :

$$W(s) = \begin{cases} W_f & 0 < s < s_1 \\ ((s - s_2)/(s_1 - s_2))\, W_f + ((s - s_1)/(s_2 - s_1))\, W_n & s_1 < s < s_2 \\ 0 & \text{otherwise} \end{cases} \tag{9}$$

where W_f is the average flank wear on the flank edge, W_n is the nose wear at the end point s_2, and s_1 is either the s value of the tangent point connecting the flank edge and the nose edge when greater than zero, or is zero otherwise.

By substituting Eqs. (6-9) into Eqs. (4) and (5), the following simplified model for the change of the cutting force is obtained.

$$\vec{F}_p = P_{av} \int_0^{s_2} W(s)\, \vec{n}(s)\, ds \tag{10}$$

$$\vec{F}_f = \frac{1}{2} \mu\, P_{av} \left[W_n (s_2 - s_1) + W_f (s_2 + s_1) \right] \vec{v} \tag{11}$$

Note that $\vec{F}_p$ actually consists of a component in the radial cutting force direction and a component in the feed cutting force direction, and $\vec{F}_f$ is almost in the normal cutting force direction (with a negligible amount in the feed cutting force direction.)

If we denote $\triangle\vec{F}_r$, $\triangle\vec{F}_d$, and $\triangle\vec{F}_n$ as the radial, the feed, and the normal components which constitute the total cutting force change due to the clearance wear, the relationships between them and $\vec{F}_p$ and $\vec{F}_f$ may be written as

$$\vec{F}_p = \Delta\vec{F}_r + \Delta\vec{F}_d \tag{12}$$

and

$$\vec{F}_f = \Delta\vec{F}_n. \tag{13}$$

Note that these equations are vector equations.

When compared with Eqs. (10) and (11), the magnitude of these three components may be expressed as

$$|\triangle\, \vec{F}_r| = P_{av}\, \mathcal{F}_r(s) \tag{14}$$

$$|\triangle\, \vec{F}_d| = P_{av}\, \mathcal{F}_d(s) \tag{15}$$

Table 1: The cutting conditions of the three experiments.

<table>
<tr><th>Exp. No.</th><th>Insert</th><th>Depth of cut (in)</th><th>Feed (in/rev)</th><th>Cutting speed (ft/min)</th></tr>
<tr><td>1</td><td rowspan="3">TPG
434
G370</td><td rowspan="3">0.1</td><td>0.006</td><td>800</td></tr>
<tr><td>2</td><td rowspan="2">0.004</td><td rowspan="2">1200</td></tr>
<tr><td>3</td></tr>
</table>

and

$$|\triangle \vec{F}_n| = \frac{1}{2}\,\mu\, P_{av}\, \mathcal{F}_n(s) \tag{16}$$

where $\mathcal{F}_r(s)$ and $\mathcal{F}_d(s)$ are the radial and the feed components of the integral in Eq. (10), and $\mathcal{F}_n(s)$ is the function to the right of P_{av} in Eq. (11). These $\mathcal{F}$ functions can be evaluated for a specific cutting tool geometry and cutting conditions, and therefore may be considered as known values.

Experiments were conducted to test the simplified model given in Eqs. (10) and (11). Since the crater wear is not considered in this model, it is desired to cut by using inserts with clearance wear only. Tools with artificial flank wear were used by a few researchers for this purpose [1,4]. However, we have found that it is almost impossible to grind an insert to have a clearance wear with the natural wear shape when the insert nose is also involved in the cutting. As an alternative, by assuming that crater wear develops slower than clearance wear [5] and has a negligible effect on the cutting force at the initial period of cutting, we can examine the cutting force behavior at this period for testing the model. An insert with a relief angle of 11 degrees was chosen for the cutting operation in order to avoid the possible rubbing of the insert nose against the finished workpiece (which is not considered in the model).

Three experiments were conducted. The cutting conditions are listed in Table 1. Notice that experiments #2 and #3 are identical. The measured cutting forces of the first two experiments are shown in Figs. 3-4. The first cutting periods are used to verify the simplified model. The measured W_f and W_n after the first cut in each experiment are listed in Table 2.

In order to calculate the force-component changes based on the simplified model, P_{av} and μ should be given. These values, however, are not known. Nonetheless, the ratio of the radial cutting force component change, $|\triangle \vec{F}_r|$, to the feed component change, $|\triangle \vec{F}_d|$, may be computed by deviding Eq. (14) by Eq. (15) which cancels the unknown P_{av}. To verify the model, the calculated ratio is compared with the actual measured value (given in Table 2) for the three experiments. As one may see, the predicted values are close to the measured values, but always a little bit higher. (The speculated reason is that the chip is thicker on the flank cutting edge and causes more residual pressure on the flank wear surface than on the nose wear surface [6]. Therefore, the feed component of the cutting force increases more than the predicted value and drives the measured ratio

Table 2: The measured clearance wears, the ratios of the radial cutting force component change to the feed component change, and the estimated friction coefficients.

Exp. No.	W_n (in)	W_f (in)	Predicted ratio	Measured ratio	Estimated μ
1	0.002	0.002	0.65	0.48	0.44
2	0.002	0.003	0.53	0.45	0.42
3	0.002	0.0035	0.50	0.41	0.42

down.)

If the pressure distribution is taken as a constant, the friction coefficient may be computed from Eqs. (16) and (14) (or (15)). The calculated average values of μ are also listed in Table 2, and they appear to be reasonable and consistent in all our three experiments. The results of the ratio of the force changes and μ show that the model development is reasonable.

3 The crater wear model

The relationship between the cutting force and crater wear has also been investigated [7]. It was reported that crater wear decreases the cutting force. This may be explained by the "sharpening" of the cutting edge due to crater wear, which increases the effective rake angle, and, subsequently, decreases the cutting force. However, an accurate model, required for the purpose of tool wear estimation, is not yet available because of the complexities of the cutting mechanism and the wearing process involved. Nonetheless, the cutting force change due to the crater wear may be limited on a plane according to the model proposed below.

Since the major change caused by crater wear is the geometry change on the rake surface, it may be assumed that the change of the cutting force due to crater wear is only from the rake surface force component. The rake surface force may be further decomposed into two perpendicular components : the pressure component acting normal to the rake surface and the friction component acting tangent to the chip flow direction [6]. This implies that the rake surface force has no component perpendicular to the plane which contains the pressure component and the friction component.

When crater wear develops, resulted from the contact of the chip flow and the rake surface, the geometry change on the rake surface may be mainly along the chip flow direction and perpendicular to the rake surface. Accordingly, the chip flow direction may change only in the direction normal to the rake surface, and the plane which contains the chip flow direction and the normal of the rake surface may remain unchanged during the development of crater wear. Recalled that the rake surface force is assumed to lie on this plane, and, accordingly, it may change only on this fixed plane. The cutting force

Table 3: The degree angle between the measured chip flow directions and the flank cutting edge. (Values in ( ) are measured after the tool chips.)

Exp. No.	Cut # 1	Cut # 2	Cut #3	Cut # 4
1	73	73	75	(71)
2	71	74	(65)	
3	72	72	73	N/A

change due to crater wear, which is assumed to be equivalent to the change of the rake surface force, should, therefore, also remain on this fixed plane.

These assumptions imply that the cutting force change due to crater wear may have no component in the direction perpendicular to the chip flow direction and the normal of the rake surface. In other words, if there is any component of the cutting force change in this direction, it should be due to clearance wear. Based on this argument, it may be possible to separate the different changes of the cutting force due to these two different kinds of wear.

After each cut of the previous three experiments, the projected angles on the rake surface between the flank cutting edge and the chip flow direction were measured. They are listed in Table 3. As may be seen, the measured angles change within the measurement error range of 3 degrees. This observation supports the proposed crater wear model.

4 Tool wear estimation

In high speed cuttings, crater wear usually has an equal influence on the change of the cutting force as clearance wear does. In order to estimate tool wear based on the change of the measured cutting force, it is necessary to separate the force changes due to clearance and crater wears. In orthogonal cutting, the cutting force change due to flank wear lies on the same plane as the force change due to crater wear, and the separation of the force changes due to these two kinds of wear becomes impossible [4]. However, in oblique cutting or bar turning, the separation becomes possible because the force change due to clearance wear may lie outside the plane of the force change due to crater wear.

Let us assume that, in stead of Eq. (9), $W(s)$ may be expressed as a product of a shape function $h(s)$ and a nominal wear W_{nom}, i.e.,

$$W(s) = W_{nom}\, h(s), \tag{17}$$

where $h(s)$ satisfies

$$\left(\int_0^{s_2} h(s)\, ds\right) / \left(\int_0^{s_2} ds\right) = 1. \tag{18}$$

Since $W(s)$ is a function of time, it should be written as

$$W(s) = W(s,t). \tag{19}$$

If we further assume that the shape function $h(s)$ does not change with time, as

$$\partial h(s)/\partial t \; = \; 0, \tag{20}$$

Eq. (17) may be rewritten as

$$W(s,t) = W_{nom}(t)\, h(s). \tag{21}$$

Notice that the assumption of Eq. (20) implies that clearance wear develops proportionally on the flank and on the nose, so that the shape function may stay unchanged.

The assumption of the pressure distribution in Eq. (6) may be relaxed into

$$\left(\int_0^{W(s)} p(s,w)\, dw \right) /W(s) = P_{av}(s), \tag{22}$$

where $P_{av}(s)$ is the pressure averaged along the direction of clearance wear. Note that Eq. (22) may accommodate the different pressure distribution on the flank wear surface and on the nose wear surface as discovered when verifying the simplified clearance wear model. However, the average pressure distribution is assumed to be time invariant, which implies

$$\partial P_{av}(s)/\partial t \; = \; 0. \tag{23}$$

If we further assume the assumptions in Eqs. (7) and (8) hold, the pressure force on the clearance wear surface, formulated in Eq. (4) as

$$\vec{F}_p = \int_0^{s_2} \int_0^{W(s)} p(s,w)\, \vec{n}\,(s)\, dw\, ds,$$

may be simplified by the following procedures as

$$\begin{aligned}
\vec{F}_p \;&=\; \int_0^{s_2} \left(\int_0^{W(s)} p(s,w)\, dw \right) \vec{n_o}\,(s)\, ds && (24)\\
&=\; \int_0^{s_2} W(s,t)\, P_{av}(s)\, \vec{n_o}\,(s)\, ds && (25)\\
&=\; \int_0^{s_2} W_{nom}(t)\, h(s) P_{av}(s)\, \vec{n_o}\,(s)\, ds && (26)\\
&=\; W_{nom}(t) \int_0^{s_2} h(s) P_{av}(s)\, \vec{n_o}\,(s)\, ds && (27)\\
&=\; W_{nom}(t)\, \vec{p}, && (28)
\end{aligned}$$

where $\vec{p}$ is the result of the integration to the right of $W_{nom}(t)$ in Eq. (27), and is time invariant according to our assumptions.

The friction force on the clearance wear surface, formulated in Eq. (5) as

$$\vec{F}_f = \int_0^{s_2} \int_0^{W(s)} \mu(s,w)\, p(s,w)\, \vec{v}\, dw\, ds,$$

can also be simplified by

$$
\begin{aligned}
\vec{F}_f &= \int_0^{s_2} \int_0^{W(s)} \mu\, p(s,w)\, \vec{v}\, dw\, ds && (29)\\
&= \int_0^{s_2} \left(\int_0^{W(s)} p(s,w)\, dw \right) \mu\, \vec{v}\, ds && (30)\\
&= \int_0^{s_2} W(s,t)\, P_{av}(s)\, ds\, \mu\, \vec{v} && (31)\\
&= \int_0^{s_2} W_{nom}(t)\, h(s)\, P_{av}(s)\, ds\, \mu\, \vec{v} && (32)\\
&= W_{nom}(t) \int_0^{s_2} h(s)\, P_{av}(s)\, ds\, \mu\, \vec{v} && (33)\\
&= W_{nom}(t)\, \vec{f}, && (34)
\end{aligned}
$$

where $\vec{f}$ is the resultant vector evaluated from the terms to the right of W_{nom} in Eq. (33), and is time invariant according to the assumptions.

As a result, the change of the cutting force due to clearance wear may be written as

$$
\triangle\, \vec{F}_{cl}(t) = (\vec{p} + \vec{f})\, W_{nom}(t). \qquad (35)
$$

When only crater and clearance wears are considered, the total force change due to tool wear, $\triangle\vec{F}_m(t)$, may be measured and separated into two components due to these two kinds of wear as

$$
\triangle\, \vec{F}_m(t) = \triangle\vec{F}_{cl}(t) + \triangle\vec{F}_{cr}(t), \qquad (36)
$$

where $\triangle\vec{F}_{cr}(t)$ is the change of the cutting force due to crater wear.

Let $\vec{c}$ be the normal vector to the plane that contains the chip flow direction and the normal of the rake surface. According to the crater wear model, $\vec{c}$ should be also perpendicular to $\triangle\vec{F}_{cr}(t)$. By taking the inner product of $\triangle\vec{F}_m(t)$ and $\vec{c}$, we have the projected value $V(t)$ as

$$
\begin{aligned}
V(t) &= \triangle F_m(t) \cdot \vec{c} && (37)\\
&= c_n \,\triangle\, F_{mn}(t) \;+\; c_d \,\triangle\, F_{md}(t) \;+\; c_r \,\triangle\, F_{mr}(t) && (38)\\
&= \triangle F_{cl}(t) \cdot \vec{c} \;+\; 0 && (39)\\
&= (\vec{p} + \vec{f}) W_{nom}(t) \cdot \vec{c} && (40)\\
&= W_{nom}(t)\, (\vec{p} + \vec{f}) \cdot \vec{c} && (41)\\
&= W_{nom}(t)\, K, && (42)
\end{aligned}
$$

where c_n, c_d, and c_r are respectively the normal, the feed, and the radial components of $\vec{c}$, $\triangle F_{mn}(t)$, $\triangle F_{md}(t)$, and $\triangle F_{mr}(t)$ are the measured three components of the cutting force change, and K is the inner product of $(\vec{p}+\vec{f})$ and $\vec{c}$ and is a time invariant constant. Notice that the three components of $\vec{c}$ may be calculated from the measured chip flow direction and the normal of the rake surface. Also notice that $V(t)$ should be proportional to the nominal clearance wear $W_{nom}(t)$, and may be obtained without knowing the value of Eq. (7) and the structures of Eqs. (17) and (22).

The projected values $V(t)$ of the previous three experiments were computed and the results of the first two experiments are shown in Figs. 5-6. As one may see, the projected value gives better linear trend than either of the three measured force components. This linear trend matches well with the observed linear development of clearance wear. In Fig. 7, the projected values verse the measured average clearance wear are plotted, and it may be seen that they are linearly related as predicted by the proposed approach.

5 Conclusion

The proposed approach may be used to estimate tool wear in different levels depending on the completeness of the available information. In the lowest level, the proposed approach can signal the on-set of the accelerated clearance wear development from the calculated projected value $V(t)$, which could help make necessary adjustments to the machining process in time. In the case when the constant K may be calibrated off-line, the proposed approach can predict the nominal clearance wear, and may be used in the machine down time planning. If the shape function $h(s)$ could be obtained from the model of clearance wear development, nose wear may be estimated from the nominal clearance wear and be used for the on-line dimensional compensation. In the highest level, when the complete model of clearance wear is available (i.e. Eqs. (7), (17), and (22) are known), the force change due to clearance wear may be determined, and the force change due to crater wear can be obtained by subtracting the force change due to clearance wear from the total cutting force change due to tool wear. Crater wear may be estimated subsequently when a complete crater wear model is available.

As a conclusion, this proposed approach is a first step toward a complete tool wear estimation based on the three components of the cutting force measurement. Further researches regarding the prediction of the chip flow direction, the prediction of the clearance wear development, the pressure distribution on the clearance wear surface, and a more complete crater wear model are needed to achieve the final goal.

References

[1] Zorev, N. N., *Metal Cutting Mechanics*, Pergamon Press, 1966.

[2] De Filippi, A., and Ippolito, R., "Adaptive Control in Turning: Cutting Forces and Tool Wear Relationships for P10, P20, P30 Carbides," *Annals of the CIRP*, vol. 17, 1969, pp. 377-379.

[3] Koren, Y., "Flank Wear Model of Cutting Tools Using Control Theory," *ASME J. of Engineering for Industry*, Vol. 100, No. 1, February 1978, pp. 103-109.

[4] Micheletti, G. F., De Filippi, A., and Ippolito, R., "Tool Wear and Cutting Forces in Steel Turning," *Proceedings of the CIRP International Conference on Manufacturing Technology*, Ann Arbor, Michigan, Sep. 1967, pp. 513-524.

[5] Colwell, L. V., and Mazur, J. C., "International Cooperative Research Program on Tool Wear," Air Force Technical Report, AFML-TR-66-387, Dec. 1966.

[6] Spaans, C., "An Exact Method to Determine the Forces on the Clearance Plane," *Annals of the CIRP*, vol. 15, 1967, pp. 463-469.

[7] Chryssolouris, G., Guillot, M., and Domroese, M., "An Approach to Intelligent Machining," *Proceedings of the American Control Conference*, Section WA5, Minineapolis, M.N., June 1987, pp. 152-160.

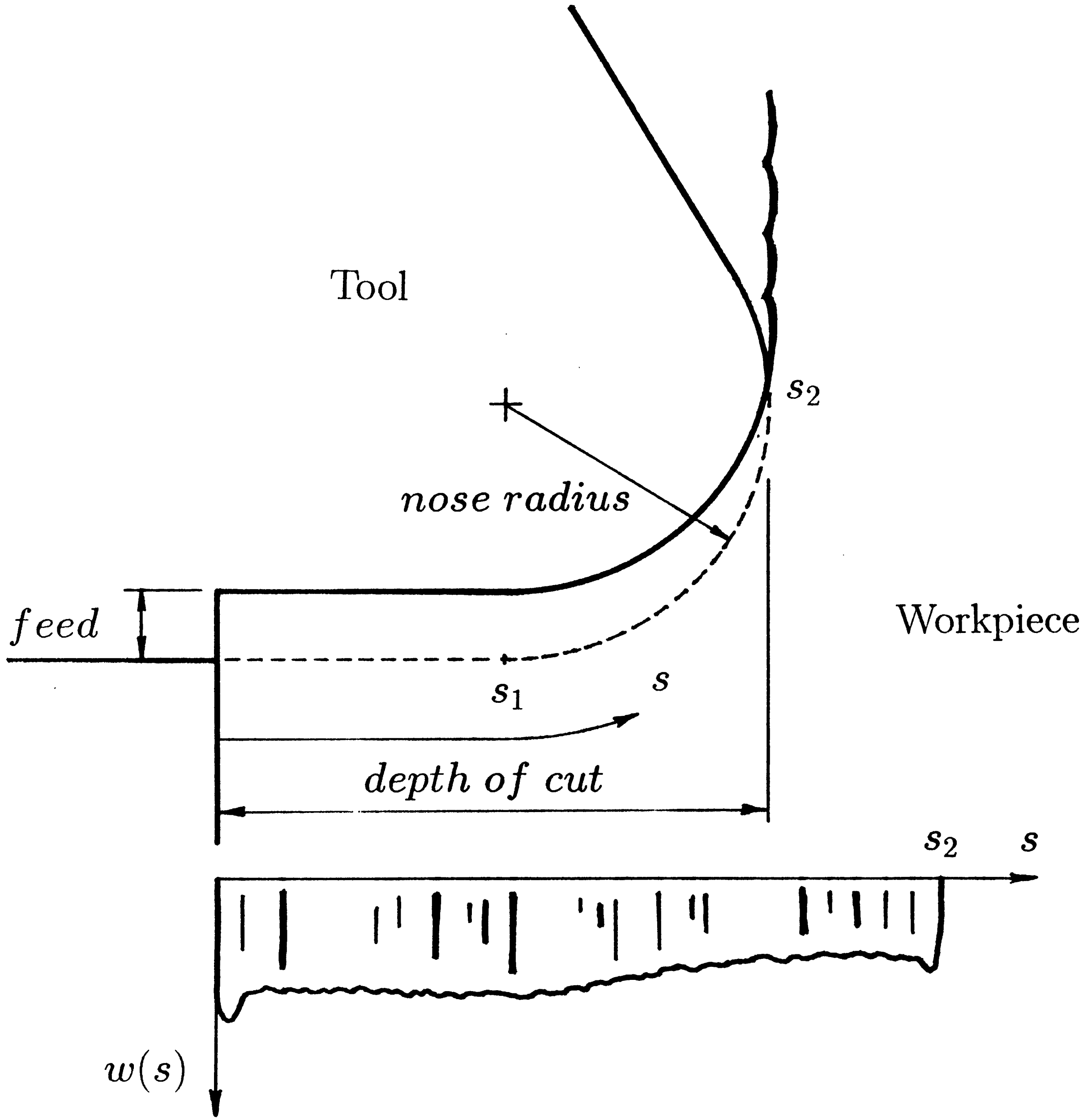

Fig.1 Schematic drawing of the clearance wear in turning operation.

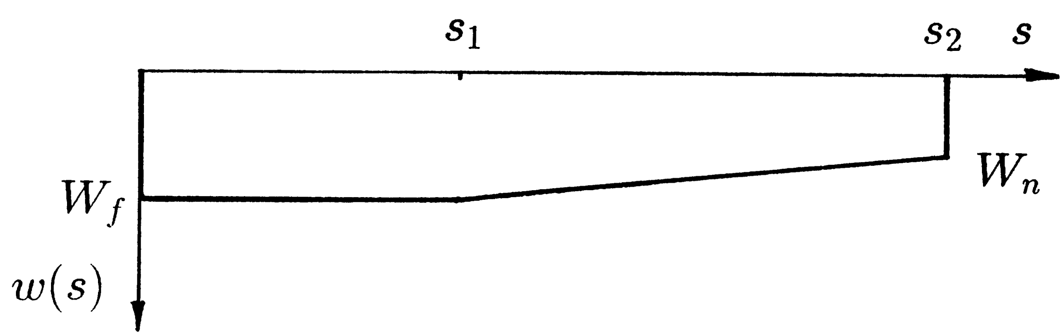

Fig.2 Graphical representation of the linear clearance wear model.

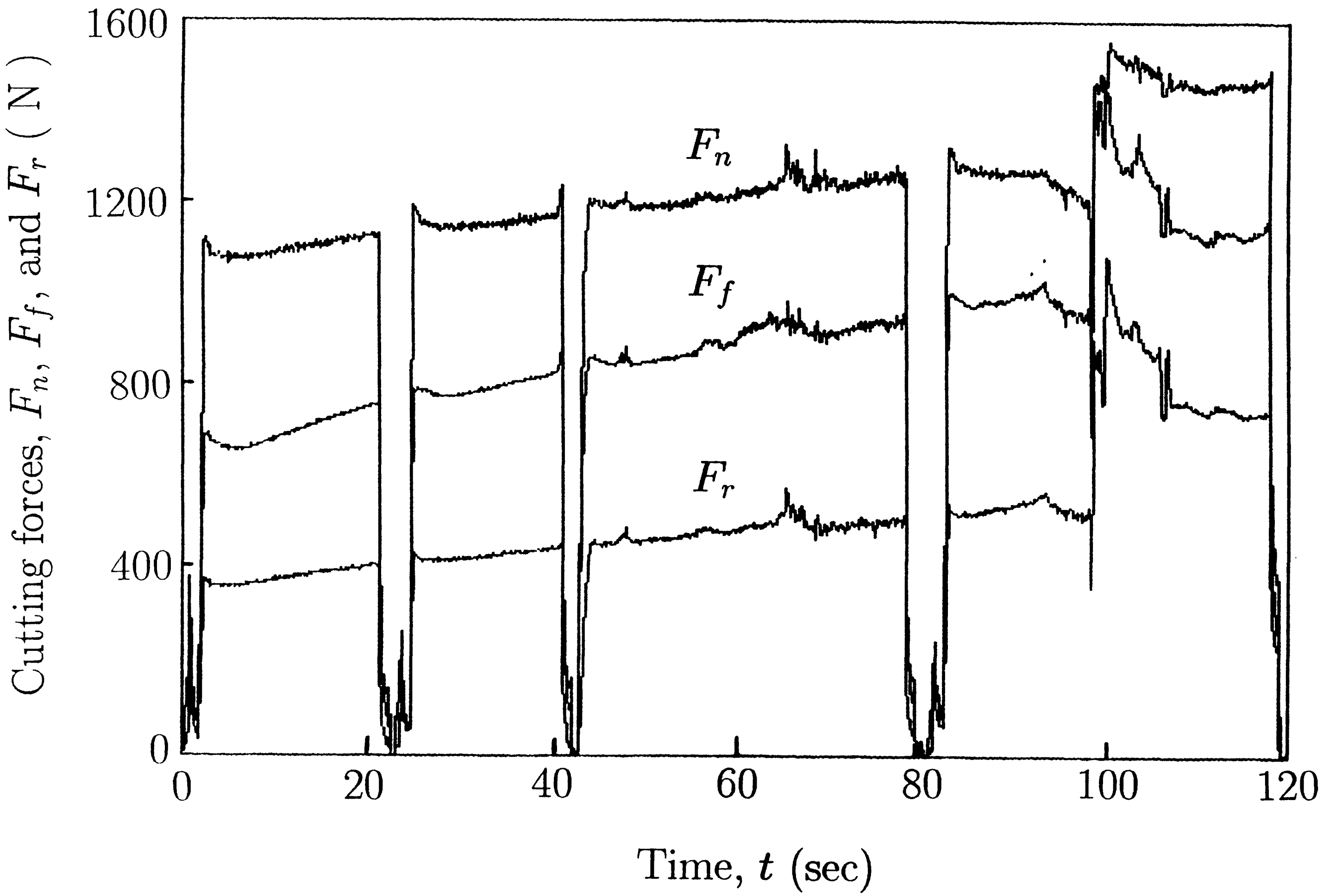

Fig.3 The measured force components of the 1st Experiment : the normal component, F_n, the feed component, F_f, and the radial component, F_r.

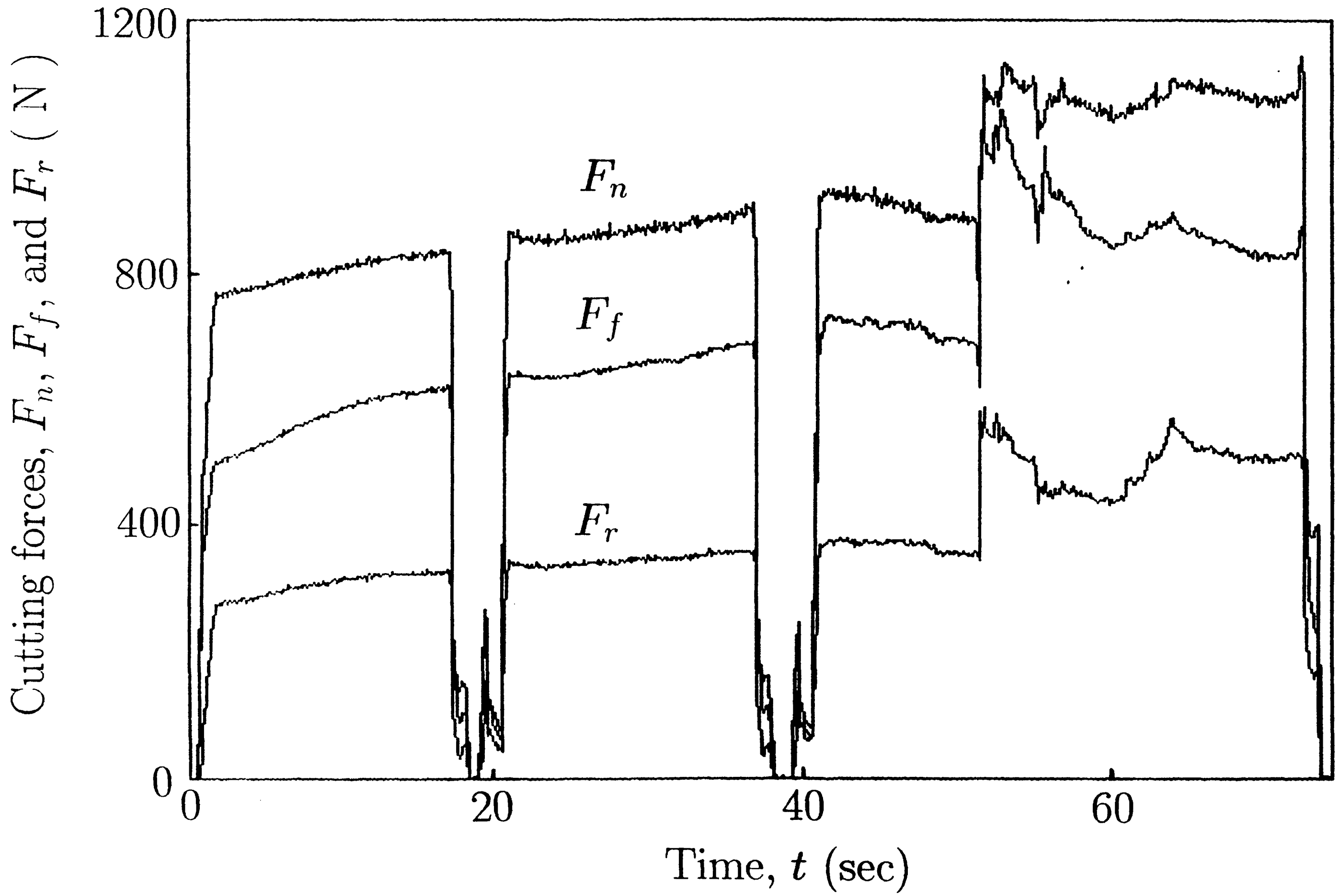

Fig.4 The measured force components of the 2nd Experiment : the normal component, F_n, the feed component, F_f, and the radial component, F_r.

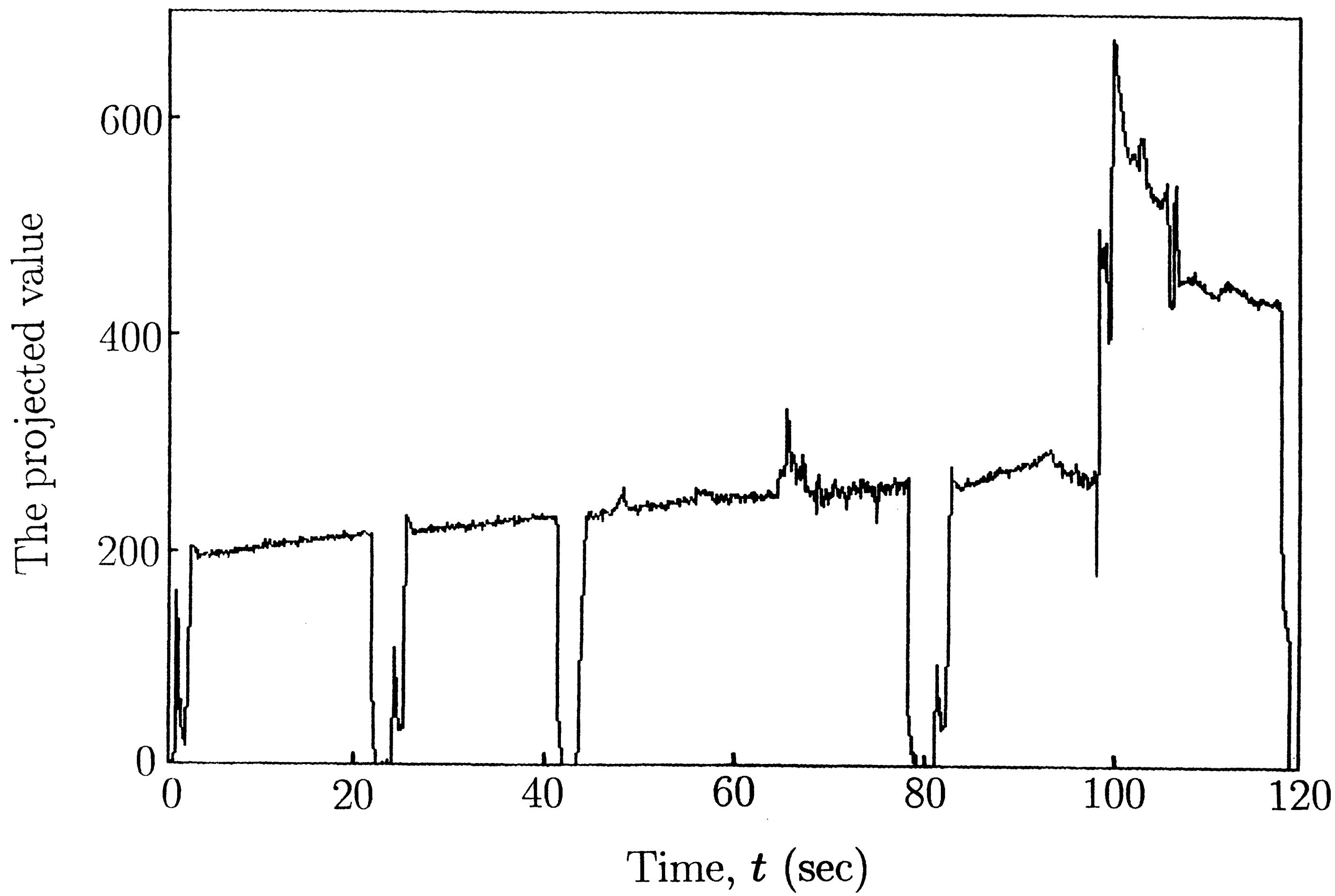

Fig.5 The projected value of the cutting force onto the normal vector of the crater wear effect plane in the 1st Experiment.

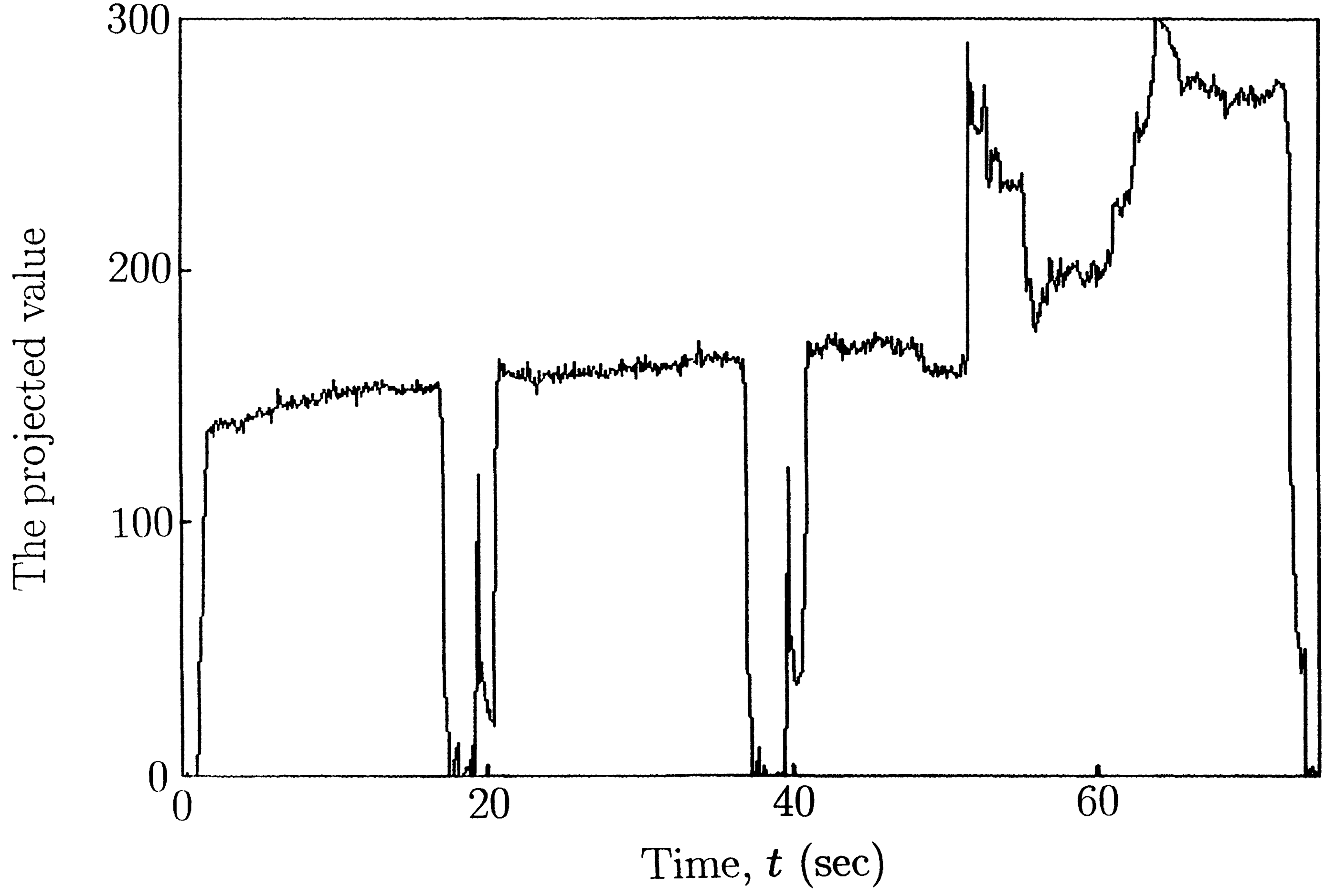

Fig.6 The projected value of the cutting force onto the normal vector of the crater wear effect plane in the 2nd Experiment.

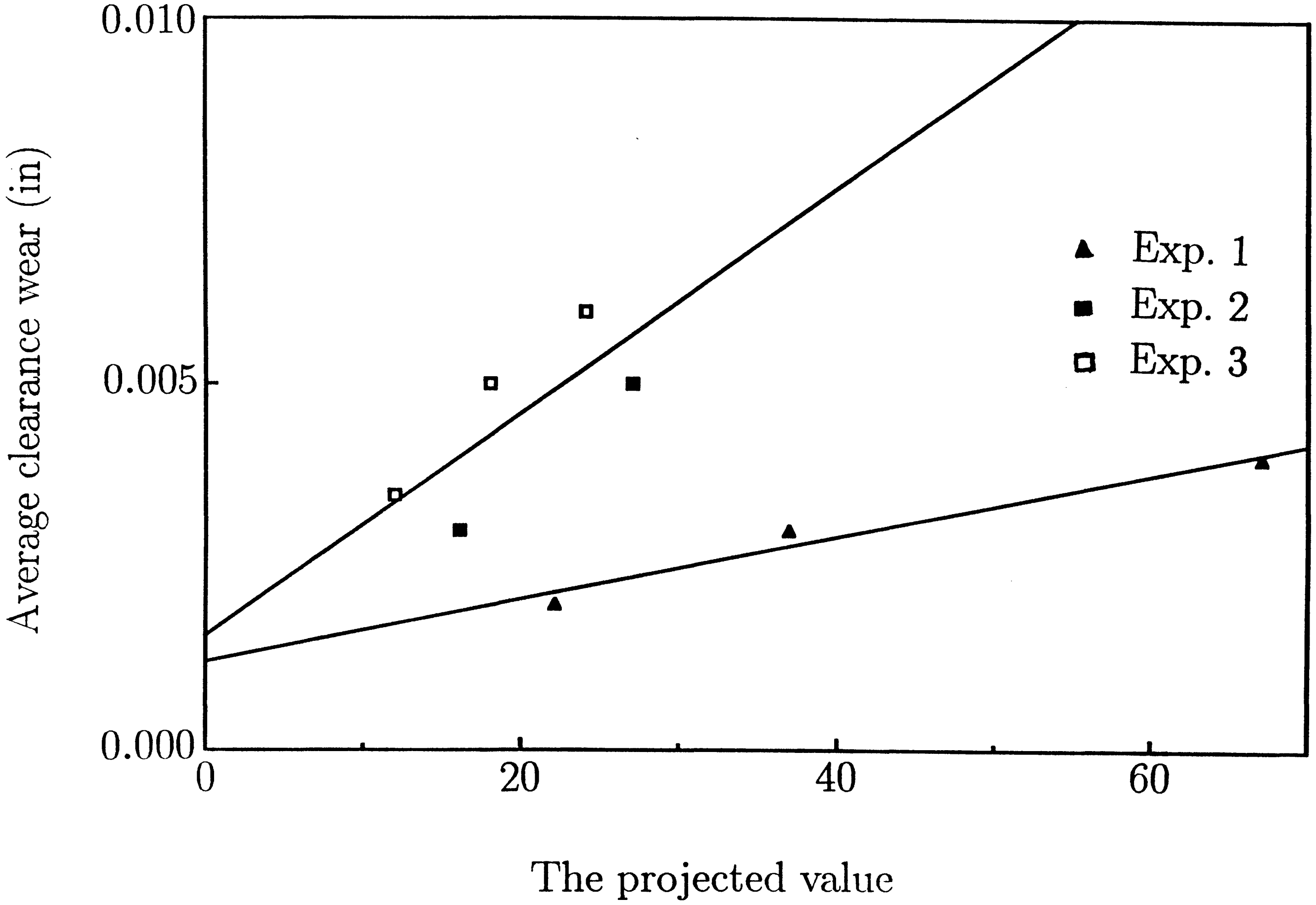

Fig.7 The projected values vs. the measured average clearance wear.